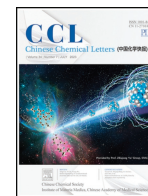




Contents lists available at ScienceDirect

Chinese Chemical Letters

journal homepage: www.elsevier.com/locate/ccllet

Electrochemical analysis of microRNAs with hybridization chain reaction-based triple signal amplification

Jianfeng Ma^a, Lingbo Gong^a, Yingying Cen^a, Lin Feng^a, Yan Su^b, Xingfen Liu^a, Jie Chao^a, Ying Wan^{b,*}, Shao Su^{a,*}, Lianhui Wang^{a,*}

^a State Key Laboratory of Organic Electronics and Information Displays & Jiangsu Key Laboratory for Biosensors, Institute of Advanced Materials (IAM), Nanjing University of Posts and Telecommunications, Nanjing 210023, China

^b School of Mechanical Engineering, Nanjing University of Science and Technology, Nanjing 210094, China

ARTICLE INFO

Article history:

Received 2 July 2022

Revised 5 November 2022

Accepted 20 November 2022

Available online 26 November 2022

Keywords:

Electrochemical

Biosensor

microRNAs

Hybridization chain reaction

Target-triggered cyclic strand displacement reaction

Triple signal amplification

ABSTRACT

Selective and sensitive detection of trace microRNA is important for early diagnosis of diseases due to its expression level related to diseases. Herein, a triple signal amplification strategy is developed for trace microRNA-21 (miRNA-21) detection by combining with target-triggered cyclic strand displacement reaction (TCSDR), hybridization chain reaction (HCR) and enzyme catalytic amplification. Four DNA hairpins (H1, H2, H3, H4) are employed to form an ultralong double-strand DNA (dsDNA) structure, which is initiated by target miRNA-21. As H3 and H4 are labeled with horseradish peroxidase (HRP), numerous HRPs are loaded on the long dsDNA, producing significantly enhanced electrocatalytic signals in the hydrogen peroxide (H₂O₂) and 3,3',5,5'-tetramethylbenzidine (TMB) reaction strategy. Compared with single signal amplification, the triple signal amplification strategy shows higher electrochemical response, wider dynamic range and lower detection limit for miRNA-21 detection with excellent selectivity, reproducibility and stability. Taking advantage of the triple signal amplification strategy, the proposed electrochemical biosensor can detect miRNA-21 in 10 HeLa cell lysates, suggesting that it is a promising method for fruitful assay in clinical diagnosis.

© 2023 Published by Elsevier B.V. on behalf of Chinese Chemical Society and Institute of Materia Medica, Chinese Academy of Medical Sciences.

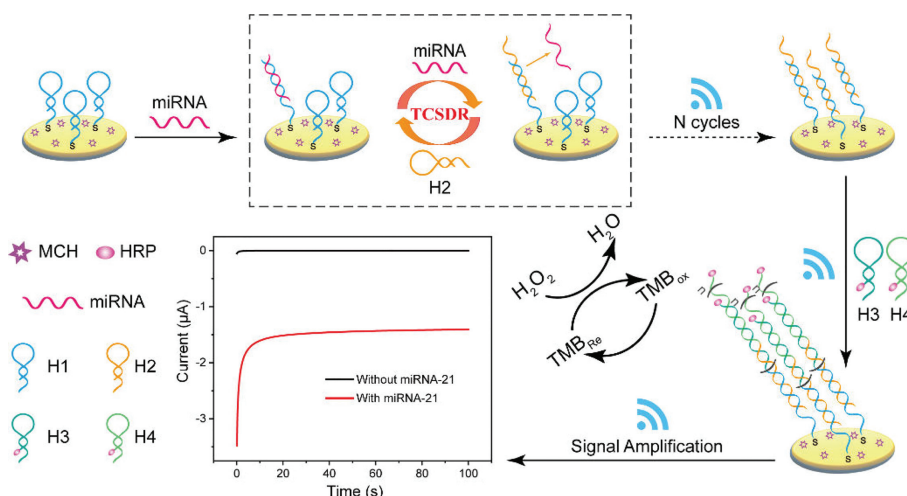
Early diagnosis of tumors is crucial for the prevention and treatment of cancerous diseases. As a potential non-invasive biomarker, many studies have proved that the expression level of microRNA (miRNA) is closely related to the occurrence and development of various tumors [1–5]. Traditional detection methods including microarrays [6], northern blotting [7] and polymerase chain reaction (PCR) [8] have been proved as useful tools to detect microRNA. However, some drawbacks such as high-cost, time-consumption, complexity, and low sensitivity [6,9–11], greatly limit their application in fast, highly sensitive and on-site detection. Biosensor is a promising method to analyze trace microRNA with high sensitivity and selectivity coupled with different analytical techniques, including fluorescence [12,13], colorimetry [14], surface plasmon resonance (SPR) [15], surface-enhanced Raman scattering (SERS) [16], electrochemiluminescence (ECL) [17], and electrochemistry [18]. Among them, electrochemical biosensors have attracted widespread attention due to the advantages of simple,

fast, high sensitivity, high selectivity, easy miniaturization and low-cost [19–22]. To further improve the analytical performance, different amplification strategies have been introduced into construction of electrochemical biosensors, such as strand displaced amplification (SDA) [23], hybridization chain reaction (HCR) [24–26], rolling circle amplification (RCA) [27], catalyzed hairpin assembly (CHA) [28–30], etc. However, single signal amplification strategy does not meet the needs for fmol/L even amol/L miRNA detection. Therefore, rational design of multiple amplification strategies gradually attracted numerous attention due to their extraordinary signal amplification efficiency. Wei *et al.* developed a dual signal-amplification platform for microRNA-141 detection by combining with HCR and CHA, leading to a low detection limit down to 0.3 fmol/L [26].

In this study, we developed an electrochemical biosensor coupled with a triple signal amplification strategy for ultrasensitive detection of miRNA-21. Combined with the target-triggered cyclic strand displacement reaction (TCSDR), HCR and enzyme catalytic amplification, four hairpins (H1, H2, H3, H4) were initiated by target miRNA-21 to form an ultralong double-strand DNA (dsDNA) on electrode surface. Horseradish peroxidase (HRP) assembled on

* Corresponding authors.

E-mail addresses: wanying@njupt.edu.cn (Y. Wan), iamsu@njupt.edu.cn (S. Su), iamlhwang@njupt.edu.cn (L. Wang).



Scheme 1. Schematic illustration of the electrochemical biosensor based on triple signal amplification.

long dsDNA *via* labeling on both H3 and H4, which can effectively catalyze $\text{H}_2\text{O}_2 + \text{TMB}$ reaction to generate a large electrochemical signal. With the assistance of triple signal amplification, this designed electrochemical biosensor can detect as low as 0.14 amol/L miRNA-21 with a wide dynamic range of 1 amol/L–10 nmol/L. The excellent analytical performance proved that the proposed electrochemical biosensor is a powerful platform for ultrasensitive miRNA quantification in bioanalysis and clinical diagnosis.

The principle of the designed electrochemical biosensor is exhibited in Scheme 1. First, the capture hairpin probes (H1) were assembled on the electrode surface *via* Au-S bond. The addition of target miRNA-21 opened the hairpin structure of H1 to form dsDNA *via* DNA-RNA hybridization reaction. Second, the added hairpin probe (H2) competitively hybridized with H1 to form more stable dsDNA (H2-H1) and release target miRNA-21 due to the strand displacement reaction. The released miRNA-21 continually reacted with H1 to initiate the next strand displacement reaction. At this time, the biosensor achieved the first signal amplification. Third, the formed H2-H1 dsDNA has an initiated sequence, which can trigger HCR reaction. As a result, HRP-labelled H3 and HRP-labelled H4 were successfully assembled an ultralong dsDNA on the electrode surface due to the HCR reaction, which obtained the second signal amplification. Large amounts of HRP loaded on dsDNA *via* HCR reaction can effectively catalyze H_2O_2 and TMB mixture, which was the third signal amplification (enzyme catalytic amplification). Obviously, an extraordinary electrocatalytic signal was observed in the presence of miRNA-21 due to multiple signal amplification. To prevent the $\text{TMB-H}_2\text{O}_2$ solution from being oxidized by oxygen, nitrogen (N_2) atmosphere should be maintained throughout the electrochemical process.

The feasibility of the programmed TCSDR and HCR amplification was firstly evaluated by polyacrylamide gel electrophoresis (PAGE). To avoid the degradation of miRNA-21 in gel, the same synthetic target DNA-21 was used instead of miRNA-21. As presented in Fig. 1A, H1, H2, H3, H4, DNA-21 showed clear bands from Lane 1 to Lane 5, respectively. Compared with Lane 6, new bands were obtained in Lane 7 with the reaction between H1, H2 and DNA-21, suggesting that DNA-21 triggered the TCSDR. It was noted that a band belonging to DNA-21 was observed in both Lane 5 and Lane 7 at the same height, proving DNA-21 was released and can trigger the next strand displacement reaction. In Lane 8, a thick and broad band was obtained at the height of H1, H2, H3 and H4 and almost no new bands were observed in the absence of DNA-21, indicating that H1, H2, H3 and H4 almost did not hybridize with each other. With the addition of DNA-21, many obvious bright bands could be

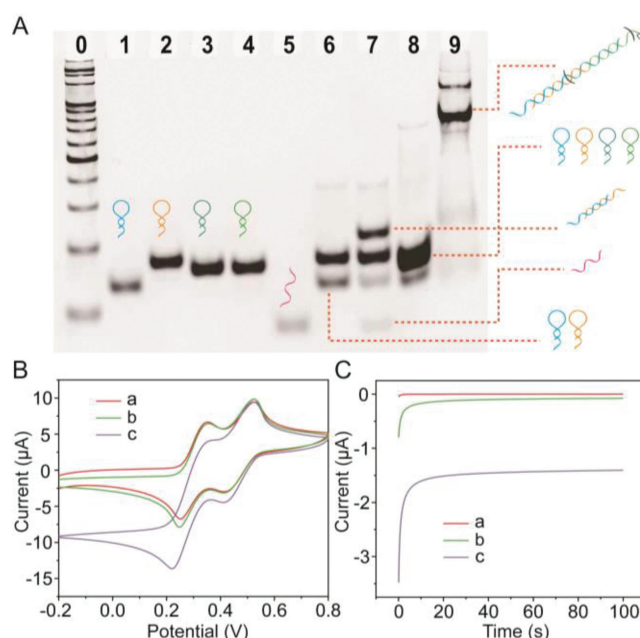


Fig. 1. (A) 8% PAGE was used to characterize the assembly of programmed TCSDR and HCR. From Lane 0 to Lane 9: 20 bp DNA ladder, H1, H2, H3, H4, DNA-21, H1+H2, H1+H2+DNA-21, H1+H2+H3+H4, H1+H2+H3+H4+DNA-21. (B) Cyclic voltammograms and (C) amperometric responses in $\text{TMB-H}_2\text{O}_2$ solution for the electrochemical biosensor in different situations: (a) H1/Au, (b) H4-H3/H2/H1/Au and (c) H4-H3/H2/miRNA-21/H1/Au.

found at the top of the lane and the bands of hairpins (H1, H2, H3 and H4) became lighter and even disappeared in Lane 9, suggesting the added DNA-21 initiated the TCSDR and HCR and the product of dsDNA was formed. Therefore, the images of PAGE suggested the designed TCSDR and HCR worked well.

The feasibility of this electrochemical biosensor for miRNA-21 detection was verified by cyclic voltammetry (CV) and chronoamperometry (*i-t*) measurements. Two pairs of well-defined redox peaks were observed at H1/Au, which was ascribed to the typical two-electron redox reaction of TMB in the presence of H_2O_2 (Fig. 1B). In the absence of miRNA-21, a few signal increase was observed at H4-H3/H2/H1/Au. This signal increase might be ascribed to the nonspecific adsorption of HRP-labelled H3 and HRP-labelled H4. Expectedly, an obvious signal increase was obtained at H4-H3/H2/miRNA-21/H1/Au with the addition of miRNA-21, which

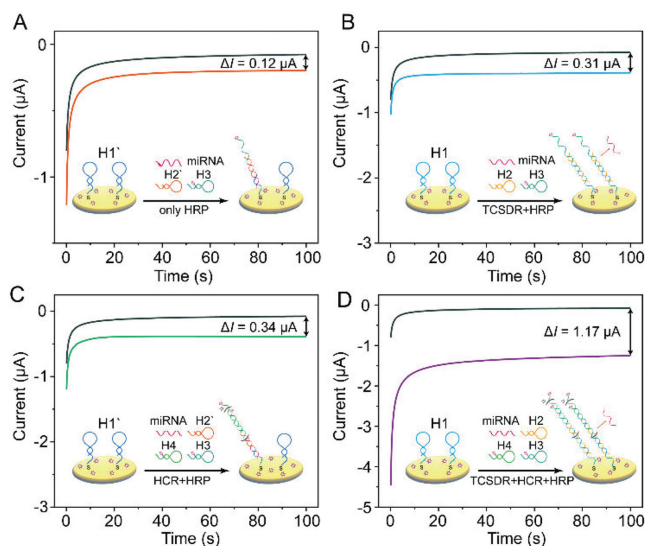


Fig. 2. Electrochemical biosensors with different signal amplification strategies in TMB- H_2O_2 solution for 100 amol/L miRNA-21 detection. (A) HRP-catalytic amplification, (B) TCSDR+HRP amplification, (C) HCR+HRP amplification and (D) triple (TCSDR+HCR+HRP) signal amplification.

was ascribed to the occurrence of TCSDR, HCR and enzyme catalytic reaction. The electrochemical signal of H4-H3/H2/miRNA-21/H1/Au was almost 1.25 times that of H4-H3/H2/H1/Au, suggesting that this designed electrochemical biosensor with multiple signal amplification can qualitatively and quantitatively determine miRNA-21. Chronoamperometry method was also used to characterize the signal amplification process [31,32]. According to the published works [33], we chose the detection potential at 150 mV. Fig. 1C showed the amperometric response of H1/Au was about 31.51 ± 0.52 nA. In the absence of miRNA-21, H1/Au incubated with H2, H3 and H4 led to a few signals increase (76.43 ± 0.91 nA), which belonged to the attribution of nonspecific adsorption. With the addition of miRNA-21, the formation of multiple signal amplification strategy made the electrochemical signal increase up to 1.44 ± 0.11 μA , which was about 44.44 times and 18.32 times higher than that of H1/Au and H4-H3/H2/H1/Au, respectively. These experimental results showed that the designed triple signal amplification platform can efficiently enhance the electrochemical response for miRNA-21 detection.

To prove the signal amplification effect of multiple amplification strategy, three control groups were designed for miRNA-21 detection, including only HRP catalytic amplification, TCSDR coupled with HRP (miRNA-21+H2+H3) and HCR coupled with HRP (miRNA-21+H2'+H3+H4) signal amplification strategies. It was noted that the H2' is different from H2, which only hybridized with miRNA-21 to form a classical sandwich structure and initiate the HCR. It can be clearly seen that the currents variation ($\Delta I = I_{\text{miRNA}} - I_{\text{no miRNA}}$) of electrochemical biosensor for 100 amol/L miRNA-21 detection was 0.12 μA of HRP catalytic amplification (Fig. 2A), 0.31 μA of TCSDR+HRP amplification (Fig. 2B), 0.34 μA of HCR+HRP amplification (Fig. 2C) and 1.17 μA of triple amplification, respectively (Fig. 2D). Obviously, the current variation of the designed biosensor for 100 amol/L miRNA-21 detection was about 9.75 times, 3.77 times and 3.44 times than that of only HRP, TCSDR+HRP and HCR+HRP amplification strategy, respectively, suggesting that the triple signal amplification has better electrochemical response than single or double signal amplification strategies.

TCSDR and HCR reaction times are important parameters to affect the performance of this biosensor for miRNA-21 detection. As

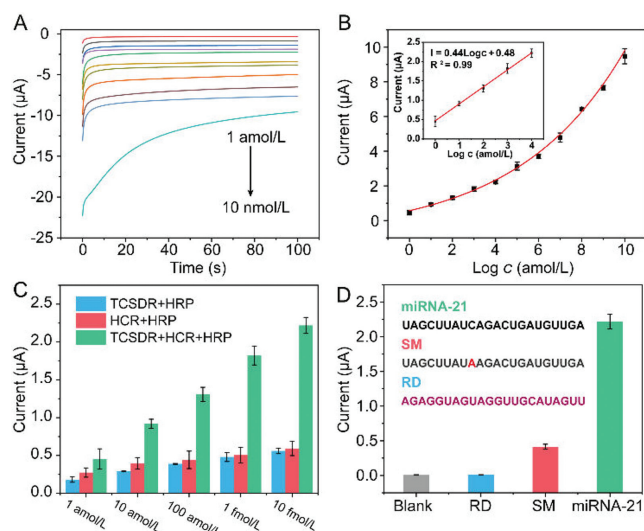


Fig. 3. (A) Amperometric responses of the biosensor for the detection of miRNA-21 with different concentrations from 1 amol/L to 10 nmol/L. (B) The corresponding amperometric signal vs. logarithmic plots of miRNA-21 concentrations. Inset: the linear calibration curve ranging from 1 amol/L to 10 fmol/L. (C) Comparison of detection performance of different signal amplification strategies. (D) The histogram of selectivity testing results from single-base mismatch sequence (SM), random sequence (RD) and target miRNA-21 at the same concentration.

illustrated in Fig. S1A (Supporting information), the electrochemical currents of this biosensor increased with the increasing incubation time ranging from 0 to 60 min. The electrochemical response reached a plateau when the incubation time was 60 min. Therefore, the TCSDR time was chosen as 60 min. Similarly, 60 min was selected as the optimal HCR reaction time (Fig. S1B in Supporting information).

According to the successful construction of the triple amplification strategy, the analytical performance of this electrochemical biosensor was investigated in H_2O_2 -TMB solution. Fig. 3A exhibited the amperometric responses of the biosensor for different concentrations of miRNA-21 detection. Obviously, the currents of this biosensor increased with the addition of 1 amol/L-10 nmol/L miRNA-21. When the concentration of miRNA-21 was from 1 amol/L-10 fmol/L, a linear calibration equation was obtained as $I = 0.44 \log(C/\text{amol/L}) + 0.48$ ($R^2 = 0.99$) with a detection limit of 0.14 amol/L ($S/N = 3$, Fig. 3B). To further prove the performance of triple signal amplification, we compared the analytical performance of triple signal amplification strategy with double signal amplification strategies for 1 amol/L-10 fmol/L miRNA-21 detection (The linear equation and detection limit were listed in Fig. S2, in Supporting information). Obviously, the biosensor with triple amplification showed larger electrochemical signal and lower detection limit than those of TCSDR-amplification and HCR-amplification biosensors, respectively, suggesting that the excellent contribution of triple signal amplification strategies in this designed biosensor for miRNA-21 detection (Fig. 3C). The analytical performances of this biosensor were better than those of other published multiple signal amplification works, which was listed in Table S2 (Supporting information). The selectivity of this biosensor was evaluated by comparing the electrochemical responses for the detection of single-base mismatch (SM) miRNA, the random (RD) miRNA and target miRNA-21. Fig. 3D showed the electrochemical response of this biosensor for miRNA-21 detection is greatly larger than those for SM and RD miRNA detection. It is almost 5.39 times and 27.63 times higher than that for SM and RD miRNA detection, respectively, indicating that this proposed biosensor has an excellent selectivity.

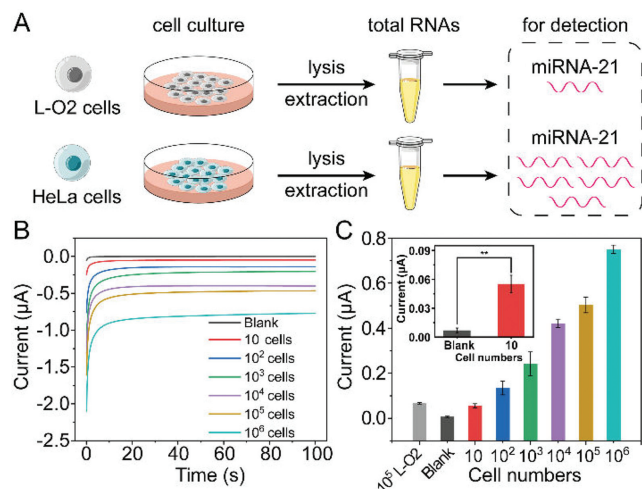


Fig. 4. (A) Schematic illustration of this biosensor for miRNA-21 detection in cell lysates. (B) Amperometric responses of this biosensor in HeLa cell lysates. (C) The corresponding currents for miRNA-21 detection in lysates of 10^5 L-O2 cells and different amount of HeLa cells. Inset: the statistical significance between 10 HeLa cells and blank (** $P < 0.01$).

The repeatability of the biosensor was investigated by using eight independently fabricated electrodes for 100 pmol/L miRNA-21 detections under the same conditions. The relative standard deviation (RSD) was calculated as about 5.49%, proving acceptable repeatability of this biosensor (Fig. S3 in Supporting information). The storage stability of this biosensor was studied by storing the developed electrodes at 4 °C in the refrigerator. The electrochemical response was tested every day. Experimental results showed only 12.09% decrease in current after weekly storage, revealing good storage stability of this biosensor (Fig. S4 in Supporting information).

On the basis of excellent analytical performance, this designed biosensor was employed to determine miRNA-21 in cells lysates (Fig. 4A). For comparison, cervical cancer cells (HeLa) cells with high miRNA-21 expression and human normal hepatocytes (L-O2) cells with low miRNA-21 expression were selected as analytical models. As shown in Fig. 4B, the electrochemical current obviously increased along with the increase of the number of HeLa cells, indicating this biosensor can successfully detect miRNA-21 expression in HeLa cell lysate. The corresponding currents for miRNA-21 detection in 10^5 HeLa cell lysates was 7.51 times that for 10^5 L-O2 cell lysates (Fig. 4C). Notably, the content of miRNA-21 in 100 HeLa cells lysates was higher than that of 10^5 L-O2 cells. Moreover, the current of this biosensor for miRNA-21 detection in 10 HeLa cells was larger than the background current, suggesting that the electrochemical biosensor can effectively determine miRNA-21 in 10 HeLa cells at least. Quantitative reverse transcription polymerase chain reaction (qRT-PCR) was used to determine the total content of miRNA-21 in the lysates from L-O2 and HeLa. The obtained results are similar to the performance of the proposed electrochemical biosensor (Fig. S5 in Supporting information). All results indicated that this biosensor has a potential application in clinical diagnosis [18,34–38].

In summary, we developed an electrochemical biosensor for ultrasensitive detection of miRNA by coupling with TCSDR, HCR and enzyme catalytic reaction. Due to the synergistic effect of the triple signal amplification strategy, this designed biosensor exhibited an ultrawide dynamic range (1 amol/L–10 nmol/L) and ultralow de-

tection limit (0.14 amol/L) for miRNA-21 detection with high selectivity, reproducibility and stability. The excellent analytical performance made this biosensor determine miRNA expression in 10 HeLa cell lysates, proving that this biosensor was of great potential in clinical diagnosis and biochemical research.

Declaration of competing interest

The authors declare no competing financial interest.

Acknowledgments

This work was supported by the National Key Research and Development Program of China (No. 2017YFA0205302), the Natural Science Foundation of Jiangsu Province-Major Project (No. BK20212012), the National Natural Science Foundation of China (No. 21874071), the “Six Talents Peak” Foundation of Jiangsu Province (No. SWYY-046) and the Priority Academic Program Development of Jiangsu Higher Education Institutions (PAPD, No. YX030003).

Supplementary materials

Supplementary material associated with this article can be found, in the online version, at doi:10.1016/j.ccl.2022.108012.

References

- [1] G.A. Calin, C.M. Croce, *Nat. Rev. Cancer* 6 (2006) 857–866.
- [2] H. Dong, J. Lei, L. Ding, et al., *Chem. Rev.* 113 (2013) 6207–6233.
- [3] A. Esquela-Kerscher, F.J. Slack, *Nat. Rev. Cancer* 6 (2006) 259–269.
- [4] L. Soleymani, Z. Fang, E.H. Sargent, S.O. Kelley, *Nat. Nanotechnol.* 4 (2009) 844–848.
- [5] P.S. Mitchell, R.K. Parkin, E.M. Kroh, et al., *Proc. Natl. Acad. Sci. U. S. A.* 105 (2008) 10513–10518.
- [6] J.M. Lee, H. Cho, Y. Jung, *Angew. Chem. Int. Ed. Engl.* 49 (2010) 8662–8665.
- [7] É. Várallyay, J. Burgyán, Z. Havelda, *Nat. Protoc.* 3 (2008) 190–196.
- [8] S.D. Fiedler, M.Z. Carletti, L.K. Christenson, *Methods Mol. Biol.* 630 (2010) 49–64.
- [9] N. Hao, P.P. Dai, T. Yu, et al., *Chem. Commun.* 51 (2015) 13504–13507.
- [10] S.S.K.A. Cissell, S.K. Deo, *Anal. Chem.* 79 (2007) 4754–4761.
- [11] W. Pan, T. Zhang, H. Yang, et al., *Anal. Chem.* 85 (2013) 10581–10588.
- [12] Z. Sun, J. Li, Y. Tong, et al., *Anal. Chim. Acta* 1221 (2022) 340136.
- [13] X. Chen, K. Xu, J. Li, et al., *Biosens. Bioelectron.* 155 (2020) 112104.
- [14] J. Sun, L. Li, S. Ge, et al., *ACS Appl. Mater. Interfaces* 13 (2021) 3645–3652.
- [15] W. Wu, X. Yu, J. Wu, et al., *Biosens. Bioelectron.* 175 (2021) 112835.
- [16] L. Jiang, Y. Hu, H. Zhang, et al., *Anal. Chem.* 94 (2022) 6967–6975.
- [17] Y. Zhang, G. Xu, G. Lian, et al., *Biosens. Bioelectron.* 147 (2020) 111789.
- [18] S. Su, Q. Sun, J. Ma, et al., *Chem. Commun.* 56 (2020) 9012–9015.
- [19] M. Negahdary, L. Angnes, *Coord. Chem. Rev.* 464 (2022) 214565.
- [20] J. Zhang, M. Hou, G. Chen, et al., *Chin. Chem. Lett.* 32 (2021) 3474–3478.
- [21] R. Bruch, M. Johnston, A. Kling, et al., *Biosens. Bioelectron.* 177 (2021) 112887.
- [22] F.T. Wang, J. Xu, Y.Y. Hou, et al., *ACS Sustain. Chem. Eng.* 10 (2022) 2673–2680.
- [23] J. Chang, W. Lv, J. Wu, et al., *Chin. Chem. Lett.* 32 (2021) 775–778.
- [24] F. Meng, W. Yu, C. Chen, et al., *Small* 18 (2022) 2200784.
- [25] G. Gao, J. Hu, Z. Li, et al., *Biosens. Bioelectron.* 209 (2022) 114224.
- [26] Y. Wei, W. Zhou, X. Li, et al., *Biosens. Bioelectron.* 77 (2016) 416–420.
- [27] T.L. Hou, L. Zhu, X.L. Zhang, et al., *Anal. Chem.* 94 (2022) 10524–10530.
- [28] P. Chen, L. Wang, P. Qin, et al., *Biosens. Bioelectron.* 207 (2022) 114152.
- [29] J. Shen, T. Li, M. Wang, B. Yao, *Sens. Actuators B: Chem.* 357 (2022) 131364.
- [30] J. Zhao, C. He, W. Wu, et al., *Talanta* 237 (2022) 122927.
- [31] Z. Ge, M. Lin, P. Wang, et al., *Anal. Chem.* 86 (2014) 2124–2130.
- [32] P. Fanjul-Bolado, M.B. González-García, A. Costa-García, *Anal. Bioanal. Chem.* 382 (2005) 297–302.
- [33] T. Hu, L. Zhang, W. Wen, et al., *Biosens. Bioelectron.* 77 (2016) 451–456.
- [34] X. Hua, J. Fan, L. Yang, et al., *Biosens. Bioelectron.* 198 (2022) 113830.
- [35] X. Jiang, C. Hao, H. Zhang, et al., *ACS Appl. Mater. Interfaces* 13 (2021) 41405–41413.
- [36] H. Zhang, M. Fan, J. Jiang, et al., *Anal. Chim. Acta* 1064 (2019) 33–39.
- [37] D. Wang, H. Zhou, F. Liu, Y. Li, *Sens. Actuators B: Chem.* 347 (2021) 130563.
- [38] M. Qing, S.L. Chen, J. Zhou, et al., *Talanta* 232 (2021) 122422.